Journal of Hydroscience and Hydraulic Engineering
Vol.21, No.1 May, 2003, 53-62

THE EFFECT OF PLANFORM AND CROSS-SECTIONAL SHAPE ON ACCURACY OF DISCHARGE MEASUREMENT USING FLOATS

By

A. Watanabe

Department of Civil and Environmental Engineering, Graduate School of Engineering, Hiroshima University, Higashi-Hiroshima City, Japan

and

S. Fukuoka

Department of Civil and Environmental Engineering, Graduate School of Engineering, Hiroshima University, Higashi-Hiroshima City, Japan

and

W. Takatsugu

Taisei Corporation, Nagoya City, Japan

and

H. Sakamoto

Water Resources Development Public Corporation, Ibi-chou, Ibi-gun, Gifu, Japan

SYNOPSIS

Discharge measurement is one of the most important tools used in river planning. A widely used technique is the Lagrangian measurement by means of floats. Most rivers in Japan are compound meandering channels that have a complex flow field. In such rivers, phase differentials exist between main channels and levees, making the flow fields even more complex. Therefore, it is important to ascertain the accuracy of discharge measurement in such compound channels.

In this paper, the authors present a method of three-dimensional analysis for compound meandering channels. By using this method to assess the accuracy of discharge measurements, the authors found considerable error in the float-based measurements in channels which have the aforementioned phase differential.

When carrying out discharge measurement using floats in a compound meandering channel, measurement should be limited, as much as possible, to sections in which the levees are straight. Where the levees do meander, measurements should be limited to areas where no phase differential exists; areas where a phase differential exists should be avoided. In the measuring of discharge in a compound meandering channel which has meandering levees, attention must be paid to the motion of floats in the floodchannel and near the boundary between the floodchannel and the main channel. Even greater care is called for when dense vegetation exists in the channel.

In conclusion, in cases of complex channel conditions, this proposed computational method can improve the reliability of float-based discharge measurement. This error may be reduced by using a larger number of floats in measurement.

INTRODUCTION

River discharge is one of the most important quantities used in river planning. Establishing a technique for accurately determining discharge—particularly flood discharge—is therefore of vital importance.

Measuring discharge by means of floats is a widely used technique because of its simplicity and because there is no suitable substitute. In float-based discharge measurement, the element cross-sectional discharge is determined from the product of the floats' velocity of movement and the area of the element cross-sections through which the floats move; this is then integrated over the entire river width. Most rivers in Japan have a compound cross-sectional shape consisting of a main channel and a floodchannel. In a compound meandering channel (1), (6), flood flows in the floodchannel follow the levees, whereas flows in the main channel below the floodchannel level follow the main channel. Consequently, the accuracy of flood discharge measurements obtained by using floats depends on factors such as the selection of observation sections, the manner in which floats move, and the number of measurement points. It is therefore necessary to assess the accuracy of discharge measurement hydraulically.

Fukuoka et al. (5) examined the accuracy of discharge measurements obtained by Eulerian and Lagrangian methods of observation based on flow fields given by a three-dimensional numerical analysis (2) in a flat fixed-bed compound meandering channel. The results showed that error in discharge measurement is smallest at the section of maximum radius of curvature; that large error can occur at inflection points depending on the combination of velocity and observation section; and that Lagrangian flood discharge measurement using floats affords in principle a high degree of accuracy, which, in the case of compound meandering channels which have straight levees, is almost unaffected by the method by which element cross-sections and channel section length are selected.

However, because the compound meandering channel used in the previous investigation had straight levees, flows in the floodchannel were also straight, thus creating conditions in which error in discharge measurement was less likely to occur. In a more typical planform wherein the levees also meander and have a phase differential relative to the main channel (3), path lines tend to be concentrated in fast-moving areas, increasing the likelihood of overestimation of the surface area represented by the high-velocity path lines.

The authors therefore applied a three-dimensional numerical analysis to their earlier experimentation in which a levee–main channel phase differential existed (3), and found that the calculated solution exhibited sufficient accuracy to assess Lagrangian measurements. The results were then used to determine the impact of phase differential between the levees and the main channel on the accuracy of discharge measurement using floats.

METHOD OF ANALYSIS

Object of Analysis

Table 1 lists the cases for which analysis was performed. In the channel used, the inter-levee distance was 1.7 m, the main channel width 0.5 m, the floodchannel height 0.045 m, levee sinuosity 1.04, main channel sinuosity 1.17, and slope 1:600.

Method of Analysis

Table 1. Object of analysis

Case	Main channel sinuosity	Levee sinuosity	Phase differential	Relative depth
Case1	1.17	1.04	Leading by π/2	0.49
Case2	1.17	1.04	Lagging by π/2	0.49
Case3	1.17	1.04	None	0.49

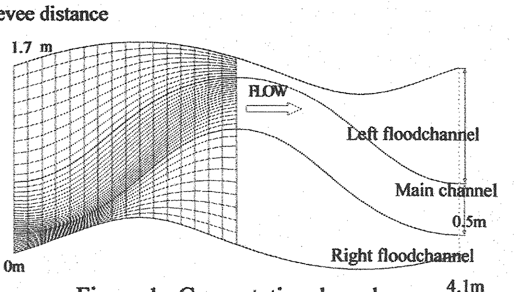

Figure 1. Computational mesh

Because the three-dimensional models used in flow field analysis have already been reported (2), (4), (5), only the main points are summarized here. A section is analyzed here which corresponds to one wavelength of main channel meander in the aforementioned compound meandering channel. Because of the periodicity of the channel boundary shape, spectral expansion was performed using cyclic boundary conditions in the longitudinal direction in the section. The computational mesh of spectral points used in the analysis (see Figure 1), used a general curviliear coordinate system and consisted of 32 longitudinal partitions, 39 lateral partitions, and nine vertical partitions (five of which were below floodchannel level).

Equations of motion (Eqs. 1, 2 and 3 in the appendix) and continuity equations (Eq. 5) were used for flow field analysis. The pressure field was determined with a SMAC scheme, and the velocity and water level change spectra were time integrated using a second-order-accurate Heun time integration scheme. The coefficient of eddy viscosity was shown as Eq. 4.

COMPARISON OF ANALYTICAL SOLUTIONS AND EXPERIMENTAL VALUES

Although findings of previous research (2), (3), (4) have verified that the three-dimensional numerical analysis model predicts the flow properties of compound meandering channels extremely well, the cases discussed herein involve even more complicated channel alignments than those used in previous research. Therefore, this section compares the computed solutions with the corresponding experimental values for each case and demonstrates that the computed results are sufficiently accurate to assess the accuracy of discharge measurements in various shaped channels.

The details are discussed in the next section. Lagrangian observation employs velocity vectors and depth to calculate cross-sectional discharge. In this section, the reproducibility of depth and velocity fields is examined. Our discussion is limited to Cases 1 and 2 because a considerable effect on planform was apparent in these cases. Comparisons of experimental and computed results are shown in Figures 2, 3 and 4.

Water Level Contours

Figures 2 and 3 show the water level contours for Cases 1 and 2. The computed results reproduce the characteristically dense concentration of contour lines at locations where the main channel flow enters the floodchannel (Case 1) and accurately reproduce the same tendency as the surface slope which is greater at the outer bank.

Velocity Distribution

Figure 4 shows the velocity vector diagrams for Cases 1 and 2. Here, because the effect of a phase differential is known to occur primarily in the upper layers (3) and because the path lines used in

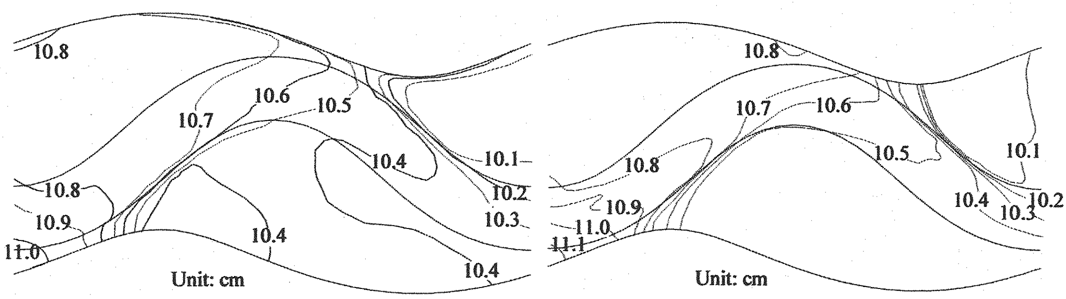

(a) Computed results (b) Experimental results

Figure 2. Comparison of experimental and computed results for water level contours in Case1

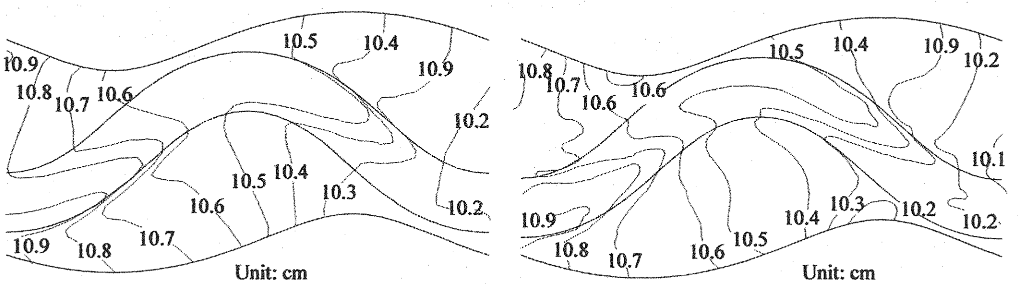

(a) Computed results (b) Experimental results

Figure 3. Comparison of experimental and computed results for water level contours in Case 2

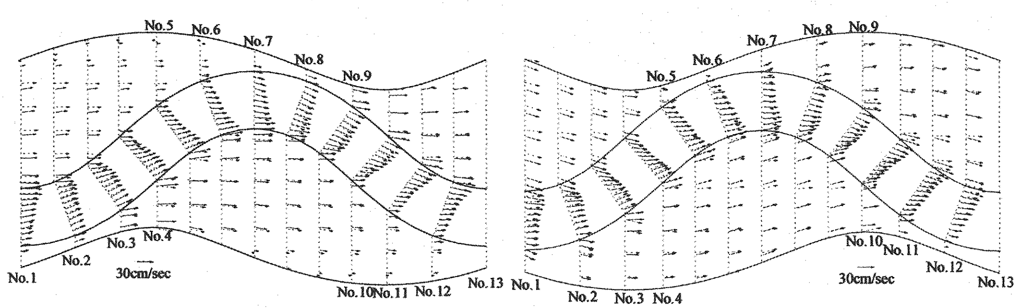

(a) Velocity above floodchannel level in Case 1 (b) Velocity above floodchannel level in Case 2

Figure 4. Comparison of experimental and computed results for flow field
(solid lines: computed results; broken lines: experimental results)

discharge calculations were determined from velocity near the surface, only velocity fields for layers above the floodchannel level are shown.

Case 1, in which the levees lead the main channel by $\pi/2$, clearly shows that a dead-water zone occurs near the crest of the levee meander, and that the floodchannel flow travels downstream rectilinearly at the meander-belt width (3). The illustrations show that the computed findings accurately depict these characteristics. Even for Case 2, the manners in which the flow characteristically disperses through the width of the channel and follows the levee (5) are also accurately reproduced. There is also good correspondence between the computational model and the experimental results with regards to main channel velocity distribution in Cases 1 and Case 2.

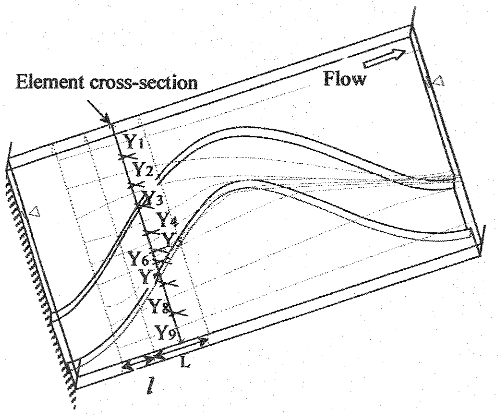

λ: Approach section
L: Observation section length
Y_n: Element cross-section width
t_n: Section passage time
v_n : Representative velocity
h_n : Representative depth

[Discharge equations]

$$v_n = L/t_n$$

$$q_n = v_n \times Y_n \times h_n$$

$$Q = \sum q_n$$

Figure 6. Model and equations for discharge calculations based on path lines

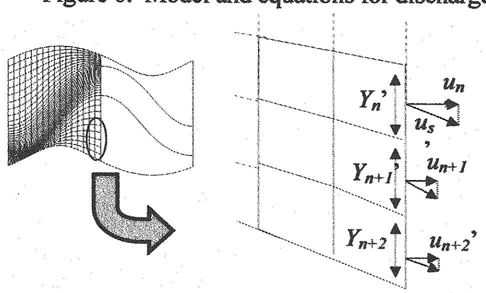

Y_n' : Computational mesh width
u_{sn}' : Velocity at assessment point
u_n' : Velocity component orthogonal to element cross-section
h_n : Representative depth

Figure 7. Definition of true discharge

LAGRANGIAN DISCHARGE MEASUREMENT

Floats are often used to measure flood discharge in rivers. However, in this Lagrangian measurement technique, the tendency of floats' paths to concentrate in high-velocity areas makes it difficult to space the floats at consistent lateral intervals. This method is thus capable of yielding only the rough and discrete velocity distribution in the lateral direction, necessitating the need to improve accuracy. In this investigation, path lines obtained computationally are considered to correspond to paths of the floats.

Method of Investigating Discharge Measurement

The method used to calculate discharge based on path lines is shown in Figure 5. The path lines themselves were calculated from near-surface velocity in order to simulate float measurement.

Representative velocity (v_n) for the observation section is obtained by dividing the section length (L) by the travel time (t_n) between the upstream cross-section of the observation section and the downstream cross-section; this value is calculated for each path line as representative velocity. In addition, a release section (i.e., where velocity of float accelerates up to that of the flow) was established to simulate actual float-based measurement. Discharge q_n for each section was calculated as the product of obtained velocity and element cross-sectional area ($Y_n \times h_n$); from the sum of these discharges, the authors calculated total discharge Q ($= \Sigma q_n$), the floodchannel discharge Q_{fp}, and the main channel discharge Q_{mc}.

The lateral width represented by a path line was basically defined as the area from the line to the midpoints between that line and those adjacent to it. A total of 11 path lines were used: five in the main

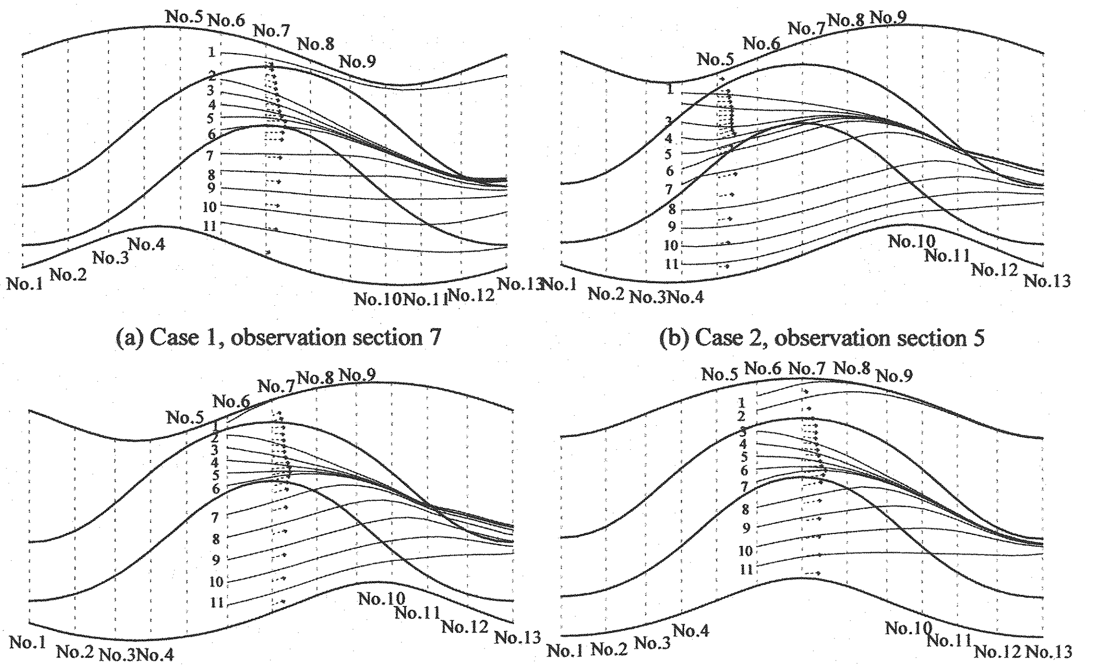

(a) Case 1, observation section 7

(b) Case 2, observation section 5

(c) Case 2, observation section 7

(d) Case 3, observation section 7

Figure 7. Path lines and velocity vectors for the observation sections

at one-half of that in the floodchannel, i.e., path lines were denser in the main channel.

Lagrangian discharge measurement assuming traces of moving floats as path lines has already been shown to be highly accurate in principle, resulting in almost no longitudinal variation in calculated discharge throughout an observation section which has straight levees (5). In this investigation, the accuracy of float-based discharge measurement affected by a phase differential between main channel and levees in a compound meandering channel is examined. These effects are discussed in the following section.

EFFECTS OF A LEVEE–MAIN CHANNEL PHASE DIFFERENTIAL ON FLOAT-BASED MEASUREMENT ACCURACY

Float Paths

Figure 7 shows the characteristic float paths and velocity vectors in the observation section for each case. Path lines are numbered sequentially starting at the left bank.

Effects of Phase Differential on Discharge Measurement Accuracy

Longitudinal variation in discharge for each case calculated as described above is shown in Figure 8; and comparisons made between true discharge and float based discharge from path lines are shown in Figure 9. True discharge is defined as the value calculated by $\Sigma\ u_n'\ (Y_n' \times h_n)$ through the measurement cross-section. Where u_n': cell's velocity component orthogonal to the cell's cross-section, and

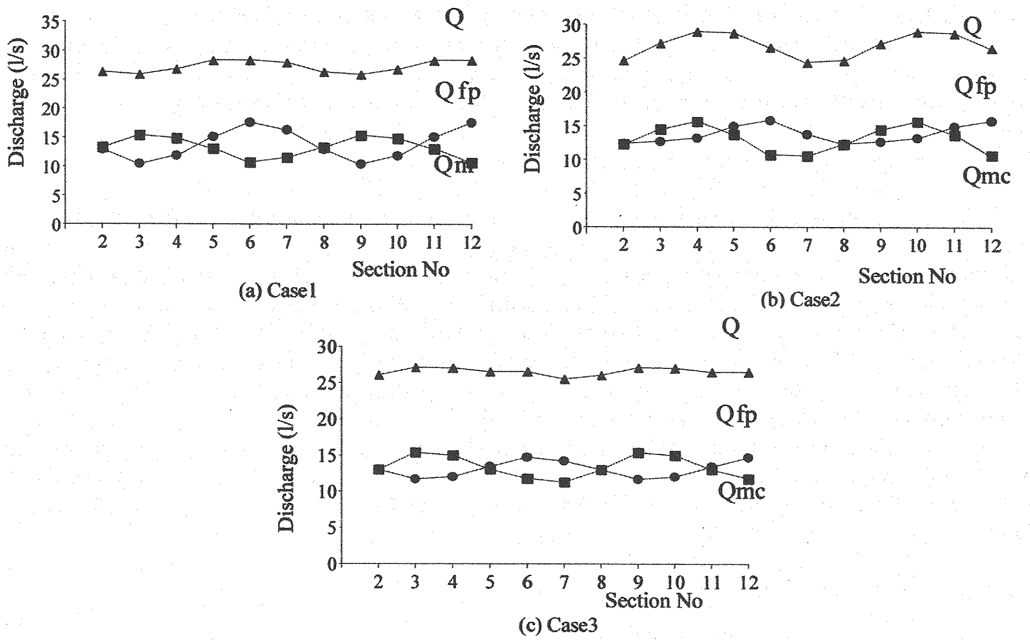

Figure 8. Longitudinal variation in discharge calculated from path lines

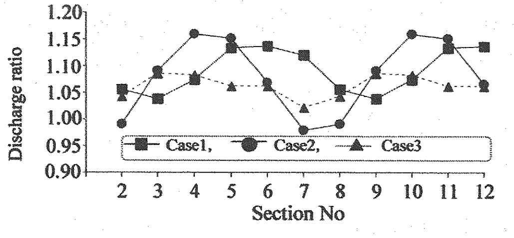

Figure 9. Comparison between true discharge and discharge calculated from path lines

($Y_n' \times h_n$): the cell's cross-sectional area in Figure 6. Discharge variation is greater in Cases 1 and 2 than when no phase differential exists, and error is as high as 13% in Case 1 and 15% in Case 2 (Figures 8 and 9). In Case 3, where no phase differential existed, variation in observed discharge is less, and error is roughly 10%. In all cases, calculated discharge was greater than observed discharge. The reasons for this error are discussed in the next section (see Figure 4 and 7).

When Levee Phase Leads the Main Channel Phase by $\pi/2$

In Case 1, error in the discharge calculated from the path lines is due to the presence of dead-water zones near the levee meander crest (Figure 4). Figure 7(a) shows the path lines for section 7, which proceeds over the dead-water zone on the left bank, but passes through an area outside the dead-water zone on right bank. It is because path line 11 representing the dead-water zone also passes through this high-velocity area in sections 5, 6, and 7 where floodchannel discharge is overestimated. This results in overestimation of total discharge (see Figure 8). Thus, the overestimation of total discharge is due to the seemingly high velocity areas near the walls represented by the closest flow lines.

When the levee phase leads the main channel phase by $\pi/2$ in float-based discharge measurement, the assessment of dead-water zones is a critical problem because including dead-water zones in effective cross-sections results in an error as high as 13% in the float based discharge measuring.

When Levee Phase Lags the Main Channel Phase by $\pi/2$

In Case 2, observed error is large in sections 4 and 5 but small in sections 7 and 8. The large error in sections 4 and 5 is due to overestimation of discharge, which occurred because the levee alignment was such that the path line 1 representing a flow along the floodchannel's left bank was concentrated in the high-velocity main channel [see Figures 7(b) and 8(b)]. In contrast, in sections 7 and 8, velocity for path line 1 (closest to the left bank) is very low because it follows the wall. Nevertheless, because the main channel path lines 2–6 are concentrated in the center of the main channel, floodchannel discharge is calculated with only path line 1 representing the flow at the flood channel's left bank, thus resulting in underestimation of discharge [see Figures 7(c) and 8(b)].

Thus, when measuring discharges in the cases where the levee phase lags the main channel phase by $\pi/2$, care is required so that a single float does not cover too wide a surface area, that is, where the flow converges on the main channel from the floodchannel or where floodchannel velocity drops abruptly near a levee.

When Levee Phase and Main Channel Are the Same

In Case 3, discharge exhibits less longitudinal variation. As seen in Figure 7(d), adjacent path lines in the floodchannel maintain constant intervals, and the effects of path line concentration are manifest only in the main channel. In addition, path lines near the levees are not too close, and floodchannel path lines are distributed at roughly equal intervals. Consequently, both longitudinal variation in discharge Q and discharge observation error are low.

CONCLUSIONS

(1) Appropriateness of Numerical Analysis

Findings of our research show that the three-dimensional numerical analysis method developed by the authors can accurately reproduce experimentally observed flow fields of compound meandering channels in which both the main channel and levees meander in differential phases.

(2) Accuracy of Float-based Discharge Measurement in Compound Meandering Channels with a Phase Differential Between the Levees and Main Channel

We were able to determine discharge according to a methodology wherein computationally obtained path lines correspond to float paths in a flow. Then, we assessed the accuracy of float-based discharge measurement with regards to planform and phase differential.

This investigation has shown that considerable error can occur if a phase differential exists between the levees and the main channel when using floats to measure discharge in a compound meandering flow having meandering levees. The variation in calculated discharge was particularly large in certain sections in the case of a levee phase leading the main channel phase by $\pi/2$. Error in both cases was due to error in floodchannel discharge calculations, which occurred because of the small number of path lines representing the floodchannel. It should be possible to improve accuracy greatly by releasing was due to error in floodchannel discharge calculations, which occurred because of the small number of path lines representing the floodchannel. It should be possible to improve accuracy greatly by releasing floats in the floodchannel at roughly the same intervals as in the main channel. When no phase differential existed between the levees and the main channel, discharge variation among observation sections was less than in the two aforementioned cases, indicating that discharge measurement by means of floats was highly accurate.

REFERENCES

1. Fukuoka, S., H. Ohgushi, D. Kamura, and S. Hirao : Hydraulic characteristics of the flood in a compound meandering channel, Journal of the hydraulic, Coastal and environmental engineering, JSCE, No.579, II-41, pp.83-92, 1997.
2. Fukuoka, S. and A. Watanae : Three dimensional analysis on flows in meandering compound channels, Coastal and environmental engineering, JSCE, No.586, II-42 pp.39-50, 1998.
3. Fukuoka, S., H. Ohgushi, and H. Okabe : Effects of sinuosity and phase between levee and main channel on the meandering compound channel flow, Annual Journal of Hydraulic Engineering, JSCE, Vol.42, pp.961-966, 1998.
4. Fukuoka, S., A. Watanabe, H. Kawaguchi, and Y. Yasutake : A study of permeable groins in Series in a straight channel, Annual Journal of Hydraulic Engineering, JSCE, Vol.44, pp.1047-1052, 2000.
5. Fukuoka, S., A. Watanabe, and W. Takatsugu : Study on the accuracy of discharge measurements in a compound meandering channel by 3-D numerical analysis, Annual Journal of Hydraulic Engineering, JSCE, Vol.45, pp.577-582, 2000.
6. Mutu, T., K. Shiono, H. Imamoto, and T. Ishigaki : 3-Dimensional structure for overbank flow in meandering channels, Annual Journal of Hydraulic Engineering, JSCE, Vol.40, pp.711-716, 1996.

APPENDIX

Governing equations

[Equation of motion in the ξ -direction]

$$\frac{Du}{Dt}=\frac{\partial u}{\partial t}+U\frac{\partial u}{\partial \xi}+V\frac{\partial u}{\partial \eta}+W\frac{\partial u}{\partial z}=g_x-\frac{1}{\rho}\left(\xi_x\frac{\partial P}{\partial \xi}+\eta_x\frac{\partial P}{\partial \eta}\right)+\nu_T\nabla^2 u+\frac{\partial}{\partial z}\left(\nu_T\frac{\partial u}{\partial z}\right) \quad (1)$$

[Equation of motion in the η -direction]

$$\frac{Dv}{Dt}=\frac{\partial v}{\partial t}+U\frac{\partial v}{\partial \xi}+V\frac{\partial v}{\partial \eta}+W\frac{\partial v}{\partial z}=g_y-\frac{1}{\rho}\left(\xi_y\frac{\partial P}{\partial \xi}+\eta_y\frac{\partial P}{\partial \eta}\right)+\nu_T\nabla^2 v+\frac{\partial}{\partial z}\left(\nu_T\frac{\partial v}{\partial z}\right) \quad (2)$$

[Equation of motion in the z -direction]

$$\frac{Dw}{Dt}=\frac{\partial w}{\partial t}+U\frac{\partial w}{\partial \xi}+V\frac{\partial w}{\partial \eta}+W\frac{\partial w}{\partial z}=g_z-\frac{1}{\rho}\frac{\partial P}{\partial z}+\nu_T\nabla^2 w+\frac{\partial}{\partial z}\left(\nu_T\frac{\partial w}{\partial z}\right) \quad (3)$$

$$\nabla^2=\left(\xi_x^2+\xi_y^2\right)\frac{\partial^2}{\partial \xi^2}+2\left(\xi_x\eta_x+\xi_y\eta_y\right)\frac{\partial^2}{\partial \xi\,\partial \eta}+\left(\eta_x^2+\eta_y^2\right)\frac{\partial^2}{\partial \eta^2}+\left(\xi_{xx}+\xi_{yy}\right)\frac{\partial}{\partial \xi}+\left(\eta_{xx}+\eta_{yy}\right)\frac{\partial}{\partial \eta}$$

Eddy viscosity

$$\nu_T=\kappa u_* z'\left(1-z'/h\right) \quad (4)$$

Continuity equation

$$\frac{\partial J'U}{\partial \xi}+\frac{\partial J'V}{\partial \eta}+\frac{\partial J'W}{\partial \zeta}=0 \quad (5)$$

NOTATION

g_x, g_y, g_z	= gravity acceleration in the x, y, z directions;
h	= depth;
$J' = x_\xi y_\eta + y_\xi x_\eta$	= Jacobian.
P	= pressure intensity;
T	= time;
u	= velocity in the x–direction;
v	= velocity in the y–direction;
w	= velocity in the z–direction (the z–axis is taken positive upward);
$U = \xi_x u + \xi_y v$	= velocity in the ξ–direction;
$V = \eta_x u + \eta_y v$	= velocity in the η–direction;
$W = w$	= velocity in the z–direction;
u_*	= shear velocity at the bed; and
z'	= height from the bed.

(Received July 31, 2002 ; revised February 10, 2003)